

## Hydrogen-free Cu: Amorphous-C: N Coating on TC4 Titanium Alloy: The Role of Gas Ratio on Mechanical and Antibacterial Potency

S. Khamseh<sup>\*1</sup>, M. Ganjaee Sari<sup>1</sup>, E. Alibakhshi<sup>2</sup>, M. Nemati Valandaran<sup>1</sup>

<sup>1</sup> Department of Nanomaterials and Nanocoatings, Institute for Color Science and Technology (ICST), P.O. Box: 16765-654, Tehran, Iran.

<sup>2</sup> Surface Coatings and Corrosion Department, Institute for Color Science and Technology (ICST), P.O. Box: 16765-654, Tehran, Iran.

### ARTICLE INFO

Article history:

Received: 5 Dec 2019

Final Revised: 22 Jan 2020

Accepted: 23 Jan 2020

Available online: 22 Feb 2021

Keywords:

Cu: amorphous-C: N

Thin coating

Magnetron sputtering

Surface properties

Antibacterial

Mechanical properties.

### ABSTRACT

*T*i-6Al-4V alloy, also called TC4, substrates are sputter-deposited by Cu: amorphous-C: N (Cu:a-C:N) thin coatings using planar magnetron sputtering physical vapor deposition device. Mixtures of argon and nitrogen at different ratios are selected as the sputtering atmosphere, and no hydrocarbon gas is used. Correlation of microstructure, morphology, surface properties, antibacterial characteristics, and mechanical performance of the coatings to the N<sub>2</sub>/Ar ratio are discussed. The outcomes from Raman spectroscopy confirm the construction of the DLC (Diamond Like Carbon) phase in the microstructure of the coatings. The thin coatings synthesized at higher N<sub>2</sub>/Ar ratios show more increased amount of sp<sup>3</sup> hybridization, improved wettability, higher internal stress, and enhanced mechanical properties, i.e., higher hardness. However, these are accompanied by lower antibacterial performance. Plastic hardness (H) value of the thin coatings increased from about 2 GPa to 13 GPa by increasing N<sub>2</sub>/Ar ratio. However, bacterial reduction percent of the thin coatings decreased from 100 to 65 % as N<sub>2</sub>/Ar ratio increased. The resultant outcomes reveal the critical role of the N<sub>2</sub>/Ar ratio on tailoring the antibacterial properties of Cu: a-C: N thin coatings as well as mechanical ones. Prog. Color Colorants Coat. 14 (2021), 281-291 © Institute for Color Science and Technology.

### 1. Introduction

The lifetime of an orthopedic part is highly dependent on the mechanical properties and tribological characteristics of its surface. For instance, even very fine scrapes created due to the wear of surface in the hip joint will lead to implant failure. Accordingly, it seems crucial to control surface wear to advance the tribological characteristics of the orthopedic parts. Surface coating of medical implants by protective coatings which are wear-resistant seems to be an

operational approach to increasing wear resistance and improving the mechanical properties [1-3]. Amorphous carbon coatings have attracted attention in biomedical applications thanks to desired characteristics, i.e. high hardness, excellent wear resistance, chemically inactiveness, and small coefficient of friction, which makes them a suitable candidate for industrial and biological applications [4-9]. There are some studies on the use of amorphous carbon (a-C) thin coatings in orthopedic joints, heart valves, coronary stents, and guide wires [10, 11].

\*Corresponding author: \* Khamseh-sa@icrc.ac.ir

It is commonly accepted that the gas composition of the plasma is a crucial parameter influencing the microstructure of the final DLC coating. It is reported that DLC coatings deposited on PET (Polyethylene Terephthalate) under  $\text{CH}_4$  plasma environment contain a collaborating deposit of high-density C–H bonds. However, when  $\text{C}_2\text{H}_2$  is used as the carbon source, amorphous carbon is generated in the coating composition [12]. Erdemir et al. [13] showed that when the H/C ratio of the source gas increases, DLC coatings show improved friction and wear resistance. It is also well accepted that nitrogen impregnation into the DLC forming plasma atmosphere is a very efficient technique to regulate the  $\text{sp}^3$  and  $\text{sp}^2$  hybridization content of the DLC coatings [14, 15]. It has been shown that Nitrogen impregnation into a-C thin coatings has an enhancing impact on mechanical properties. These coatings demonstrate higher hardness and better elasticity compared to the pristine ones [16–18]. Moreover, nitrogen-impregnated amorphous-carbon, in short form a-CN<sub>x</sub>, thin coatings show a lower friction coefficient and wear rate in wet conditions than the a-carbon thin coatings [10, 11]. However, nitrogen addition increases the residual stress and affects the coating's adhesion limiting its practical applications [19, 20]. One route proposed to overcome this problem in a-C thin coatings is to incorporate metal species into the coating [21–24]. Impregnating metal elements inside the matrix alters the coating's properties and a variety of applications becomes considerable [19, 20]. Metal incorporation greatly enhances the carbon graphitization in the coating structure and reduces surface tension [21–23]. These incorporated metals are usually divided into two categories: (i) metals that chemically react with carbon resulting in carbide clusters formation and (ii) metals without any possibilities for chemical reactions that lead to the establishment of nano-clusters of metal entrenched in the amorphous carbon matrix [25–27]. However, there exist a few studies in which the effect of metal incorporation on the mechanical characteristics of a-CN<sub>x</sub> (nitrogen entered amorphous carbon) thin coatings has been investigated [8]. From the existing literature, it seems pretty probable that incorporated metals in some cases have been able to reduce internal stresses of the coatings and simultaneously improve other characteristics like biological response and electrical properties. As an example, it is well accepted that Cu ions are incredibly

toxic to bacteria at ppb magnitudes; hence Cu is considered an antibacterial substance. This characteristic originates from the ability to release minor quantities of Cu ions to the tissues. These ions act as antiseptics/antibiotics [28, 29]. This ability mainly comes from the fact that Cu and carbon are nearly immiscible due to the relatively weak Cu-C bond energy [10, 30]. Our previous reports on Cu impregnation into a-C thin coatings revealed that internal stress decreases while plastic hardness and  $\text{H}^3/\text{E}^2$  ratio increase [21–23]. Moreover, Cu-impregnated a-C thin coatings showed super anti-corrosion performance [22]. Yu et al. showed there is a precise span of Cu concentrations across which mechanical properties and blood congeniality of the sputtered Cu/DLC coatings on magnesium substrate enhance [31]. In addition, as discussed above Nitrogen added a-C thin coatings demonstrate higher hardness, better elasticity, and lower friction coefficient and wear rate in wet conditions compared to the pristine ones. Moreover, there are some reports showing effective application of Nitrogen added a-C thin coatings in biomedical applications [1, 8].

However, there exist a few studies in which the effect of metal incorporation on the mechanical characteristics and biocompatibility of a-CN<sub>x</sub> thin coatings has been investigated. According to the author's knowledge, no study is reported on the effects of nitrogen and Cu impregnation on microstructure, mechanical, and bactericide characteristics of a-C coatings. Therefore, the current study reports microstructure, surface, mechanical and antibacterial characteristics of Cu: a-C: N thin coatings applied on TC4 alloy (Ti-6Al-4V alloy) substrates.

## 2. Experimental

### 2.1. Sputtering

A Yarenikane Saleh-DRS320 branded DC magnetron sputtering machine was employed for the application of the coatings. Ti-6Al-4V alloy, i.e. TC4, rectangles of 20 mm<sup>2</sup> surface area, and glass slides of 20 mm<sup>2</sup> surface area were used as substrates. The substrates were retained at floating potential throughout the process. Sputtering chamber pressure was  $3 \times 10^{-6}$  Torr before the initiation of the deposition process, and the length from the target to the substrates was adjusted at 110 mm. The working pressure was  $1.5 \times 10^{-2}$  Torr. A 50.8 mm diameter copper disk with 99.999% purity

was selected as the Copper target, and mixed atmospheres of Ar and N<sub>2</sub> at various ratios, i.e. N<sub>2</sub>/Ar: 0, 0.4, 1, and 2.3, were the process environment. Five graphite tablets (d = 5.08 mm and thickness = 2 mm) were homogeneously positioned on the erosion trail of the target. They act as the carbon source for the coatings. A schematic illustration of the sputtering gun and position of Cu target and graphite tablets is shown in Figure 1. The temperature of the substrate increases to about 200 °C throughout the process because of the substrate's bombardment by particles. The current and voltage of the sputtering were fixed at 0.18 A and 450 V, correspondingly, and the deposition period was set at 180 min. The variation of N<sub>2</sub>/Ar ratio and coatings thickness are summarized in Table 1.

## 2.2. Characterizations

The films structure was assessed through Raman spectroscopy by a Horiba Jobin-Yvon, LabRam HR EVOLUTION Raman spectrometer device. The Raman excitation wavelength was 532 nm. Coatings composition was chemically investigated by EPMA (electron probe micro-analyzer) apparatus (JEOL, JXA-8530F). The films thickness and surface properties were characterized by the FE-SEM technique using a FE-

SEM-model Tescan device. Surface properties were investigated through water droplet contact angle measurement utilizing an OCA 15 plus (contact angle measuring device).

*E. coli*, representative of gram-negative bacteria, was selected as the test microorganism. The specimens were first sterilized under UV irradiation. They were nursed in a BEP while mixing was applied for 10 h at 37 °C. Subsequently, the bacterial concentration was tuned at 1.0×10<sup>5</sup> CFU/mL and poured on each sample surface. Then, the test samples were nursed at 37 °C for 18 h. The viable count technique was exploited to compute the final concentration of the reference and test samples. Briefly, having accomplished the growth time, the number of colonies for each diluted sample was reckoned, and bacterial growth rate change was evaluated by equation 1.

$$R \% = \frac{B - A}{B} \times 100 \quad (1)$$

Where A (CFU/mL) is the remaining bacteria in the flask of the test sample, and B is the one for the reference sample.

The internal stress was calculated conferring to Stoney's equation by the aid of a profilometer. First, the curvature of metal strips of 5×100 mm<sup>2</sup> size was measured. Consequently, strips were positioned to a sample holder, and the sputtering process was conducted. Coated samples' curvature was once more measured, and changes due to the deposited layer were calculated. Stress,  $\sigma$ , was then evaluated through the following equation, i.e. Stoney's equation (Eq. 2):

$$\sigma = \left[ \frac{ET^2}{3(1-\nu)L^2t} \right] 4\delta \quad (2)$$

E: Young's modulus,  $\nu$ : Poisson's ratio, T: substrate thickness and L: substrate length; T: thickness of the film ( $t \ll T$ );  $\delta$ : central substrate deformation after sputtering

Mechanical characteristics, i.e. hardness and Young's modulus, were obtained by a Hysitron Inc. TriboScopes Nanomechanical Test Instrument equipped by a Berkovich diamond indenter. The measurements were all done at ambient temperature. The load was limited to an amount with which the depth of impression did not exceed 10% of the coating thickness. The latter was to eliminate the effect of the substrate.

**Table 1:** Deposition conditions and coatings thickness.

Sample code	N <sub>2</sub> /Ar ratio	Thickness (nm)
C-1	0	1500±100
C-2	0.4	1500±80
C-3	1	1500±50
C-4	2.3	1500±50

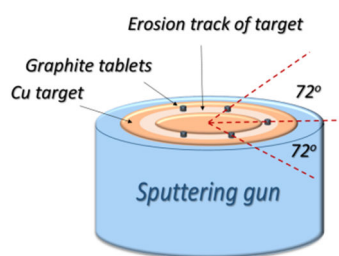


**Figure 1:** Schematic of sputtering gun and position of graphite tablets.

### 3. Results and Discussion

Change of Cu and C contents and N/C ratio of the coatings as a function of  $N_2/Ar$  ratio is plotted in Figure 2. It can be realized that Cu content decreases by increasing  $N_2/Ar$  ratio. On the contrary, C and N contents continuously increase as  $N_2/Ar$  ratio increases. To explain this behavior, it must be noted that as the  $N_2/Ar$  ratio increases, the surface of the Cu target and graphite coupons can be covered by nitride compounds, which will lead to target poisoning [32]. The target poisoning decreases sputtering yield of the Cu target and graphite coupons; hence lowers Cu and C contents in the structure of the coatings. However, the N/C ratio of the coatings decreases by increasing the  $N_2/Ar$  ratio, reaching its lowest value at  $N_2/Ar$  ratio of 1 and increases for the higher  $N_2/Ar$  ratio. Since the N/C ratio is lower than 1, Cu: a-C: N coatings with high carbon content are formed in the coatings.

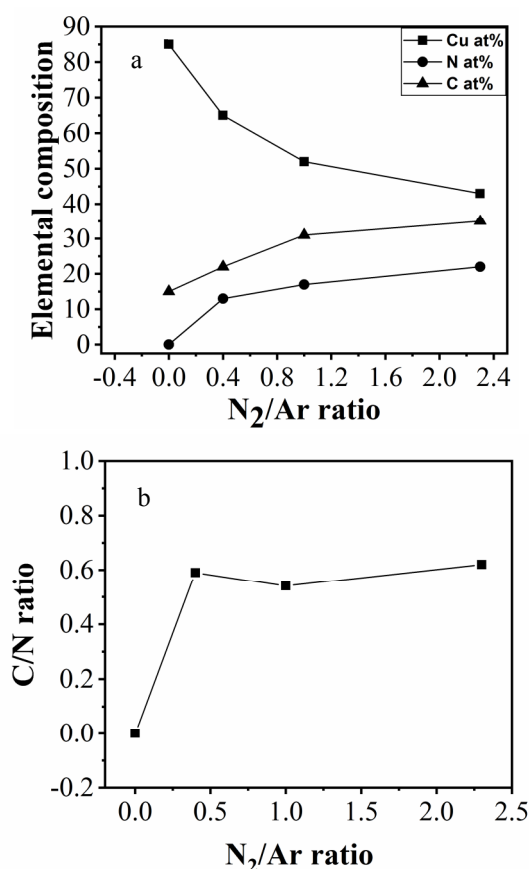


**Figure 2:** Development of the (a) chemical composition and (b) C/N ratio of Cu: a-C: N thin coatings correlated to  $N_2/Ar$  ratio.

To achieve a better apprehension of the microstructure, Raman analysis was taken into consideration. The resulted spectra for the coatings are presented in Figure 3.

Two prominent peaks in the Raman spectrum, known as D and G bands that respectively emerge across 1364 to 1387  $cm^{-1}$  and 1591 to 1595  $cm^{-1}$ , are typical features for carbon-based coatings. The defects in the structure and distortion of the lattice and the effects of dimension restriction, are correlated to D band emergence while G band (is attributed to the graphite lamellae. In other words,  $sp^3$  hybridized carbon is responsible for the D band, and  $sp^2$  hybridized carbon is in charge of the G band. The characteristics of these bands, i.e. shape, intensity ratio, and peak location, and displacement, are useful means to determine the microstructure of these coatings. To facilitate comparing, quantitative data have been extracted from Raman spectra and given in Table 2.

To define the structural orderliness of the coatings, the relative intensity of D and G bands can be exploited as a standard. To calculate the  $I_D/I_G$  ratio, the diagrams were first deconvoluted by Lorentzian fitting estimation, as can be perceived from Figure 3. Then, the intensity, i.e. the surface area of the peaks, was obtained by integrating, and the ratios were calculated. As it is depicted in Table 2,  $I_D/I_G$  ratio for the Cu: a-C: N thin coatings increases as the  $N_2/Ar$  ratio rises. This is an evidence that coatings sputtered at a higher  $N_2/Ar$  ratio also have more significant portion of  $sp^2$  carbon or bigger graphitic domain size [33, 34]. Besides, it has been shown that N incorporated amorphous carbon coatings comprise of  $sp^2$ -coordinated basal lamellae that are collapsed due to the integration of the pentagonal and cross-linked at  $sp^3$ -hybridized C sites that lead to the bending of the structural units [35]. This can also lead to an increased D peak intensity as the N content of the coatings increases. Moreover, the FWHM of the peaks likewise gives essential information on the crystallinity of the coatings. The FWHM values for D and G peaks are shown in Table 2. This parameter increases by increasing  $N_2/Ar$  ratio. This indicates that the impregnation of nitrogen into the structure of the coatings disturbs the long-range orderliness of the graphitic construction. It is commonly accepted that nitrogen incorporation improves the establishment of  $sp^2$  hybridized carbon in a-C based coating [36].

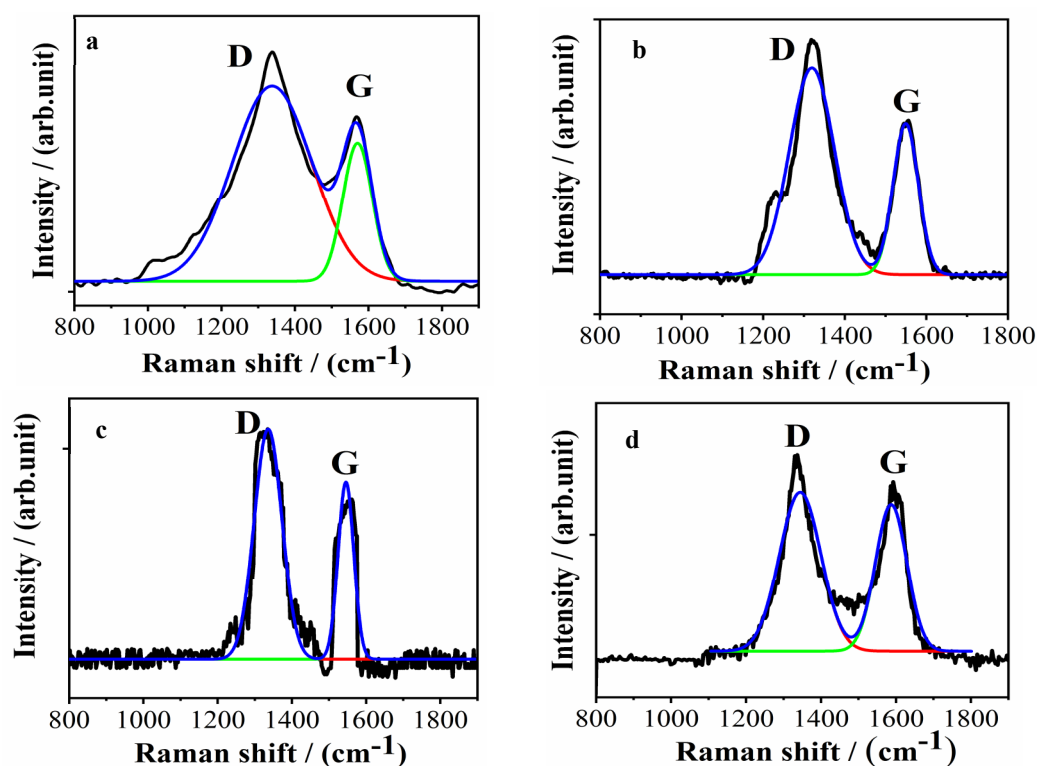


**Figure 3:** Raman spectra of Cu: a-C: N thin coatings (a-d) C-1 to C-4 thin coatings.

**Table 2:**Quantitative data from Raman spectra.

Sample code	$I_D / I_G$	D peak FWHM	G peak FWHM
C-1	1.4	75	42
C-2	2.3	111	62
C-3	2.4	131	99
C-4	3.8	218	80

To morphologically compare the coatings, the FE-SEM technique was taken into service. Images taken from the plane view of the coatings are gathered in Figure 4, with which morphology alteration upon the nitrogen flow rate is visible. For C-1 with no nitrogen in its sputtering process, a co-continuous pebble-like morphology with distinguished grain boundaries is observable (Figure 4(a)). In C-2 sputtered at  $N_2/Ar$  ratio of 0.4, the pebbles turn into blister-like

inhomogeneities that are greater in size and, of course less distinguished in grain boundaries (Figure 4(b)). For C-3 thin coating sputtered at  $N_2/Ar$  ratio of 1, a very fine grained morphology is observed that shows almost no blister-like structure and the boundaries are nearly indistinguishable (Figure 4(b)). Nonetheless, a small number of microcracks are detected on the surface of the coating. And eventually, in the C-4 thin coating applied at  $N_2/Ar$  ratio of 2.3, very smooth

surface morphology is obtained. The grains size and boundary are undetectable at this resolution of FE-SEM (Figure 4(c)).

To comprehend the correlation of the surface morphology and the physical chemistry properties of the samples, the contact angle, i.e.  $\theta$ , between a water droplet and the coatings was measured.  $\theta$  can be then correlated to surface energy. Figure 5 shows the difference in contact angle ( $\theta$ ) for the coatings. As it is depicted from the diagram, the greater the nitrogen content of the coating becomes, the lower the contact angle results. Lower  $\theta$  means better wettability by water and indicates higher surface energy for the coatings [37, 38]. Such enhanced wettability of the coating when applying on a joint replacement leads to holding the synovia on the surface and improves surface lubricity [1, 31, 39]. Moreover, this can affect the antibacterial properties of the coatings.

The ability of bacteria growth on the coatings was evaluated. The reduction in bacteria number on the various thin coatings is plotted as a function of  $N_2/Ar$  and shown in Figure 6 (a). As it can be realized, the bacteria reduction for C-1 is 100 %, that means this coating is thoroughly successful in preventing bacterial growth and suppress the colonies. However,

incorporation of nitrogen into the structure by increasing  $N_2/Ar$  ratio deteriorates this ability. The bacterial reduction of C-2, which has been applied at  $N_2/Ar$  ratio of 0.4, is 95 %. This decline is even more significant for C-3 and C-4. This indicates the bacterial growth reduction ability of the coatings decreases by increasing the  $N_2/Ar$  ratio. Conversely, the colony-forming units (CFU) increases from an average of  $2 \times 10^4$  to  $1.5 \times 10^5$  mL as  $N_2/Ar$  ratio increases (Figure 6 (b)). As was mentioned in Figure 2, the Cu content of the coatings decreases by increasing  $N_2/Ar$  ratio. The coatings containing higher amounts of Cu must logically show better antibacterial properties. Bactericide properties of Cu have been proved and accepted for decades [32]. Cu-ions are particularly toxic to bacteria at deficient concentrations (ppb scale). It was previously mentioned that is due to the releasing of small quantities of Cu-ions into the tissues [33, 34]. Also, it has been shown that a-C coatings with higher  $I_D/I_G$  ratio show better antibacterial activity [10]. As discussed previously, Cu: a-C: N coatings sputtered at higher  $N_2/Ar$  ratio have a higher  $I_D/I_G$  ratio. Hence, the antibacterial properties are seemingly determined by Cu content, and/or higher  $I_D/I_G$  ratio of the Cu: a-C: N coatings.

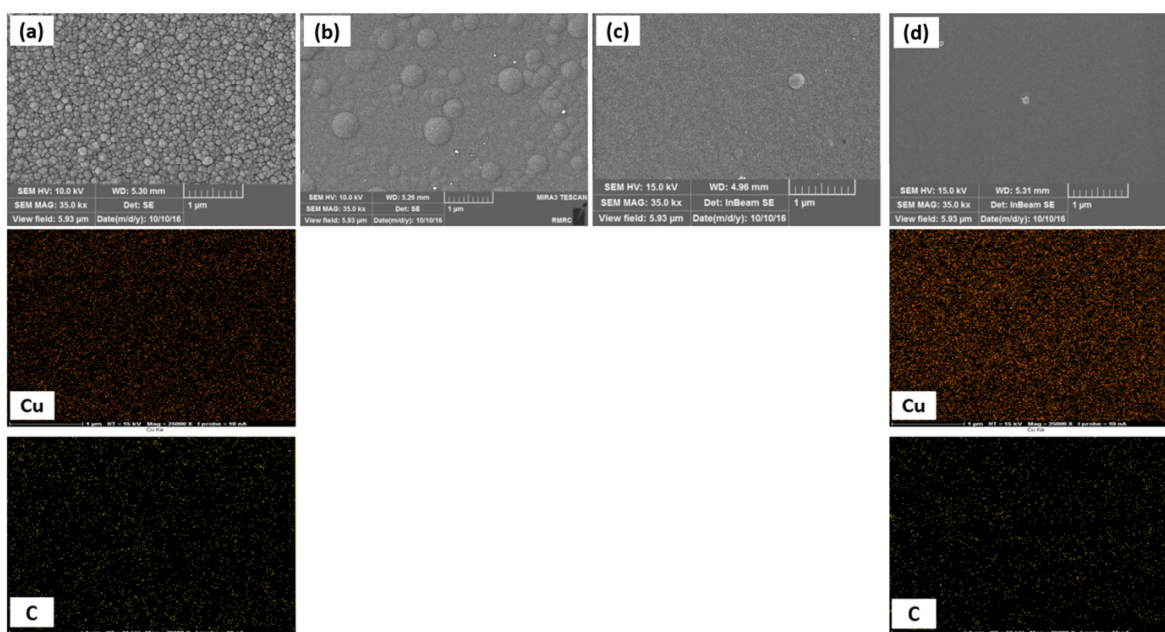


**Figure 4:** In-plane view FE-SEM micrographs and elemental map of (a-d) C-1 to C-4 thin coatings.

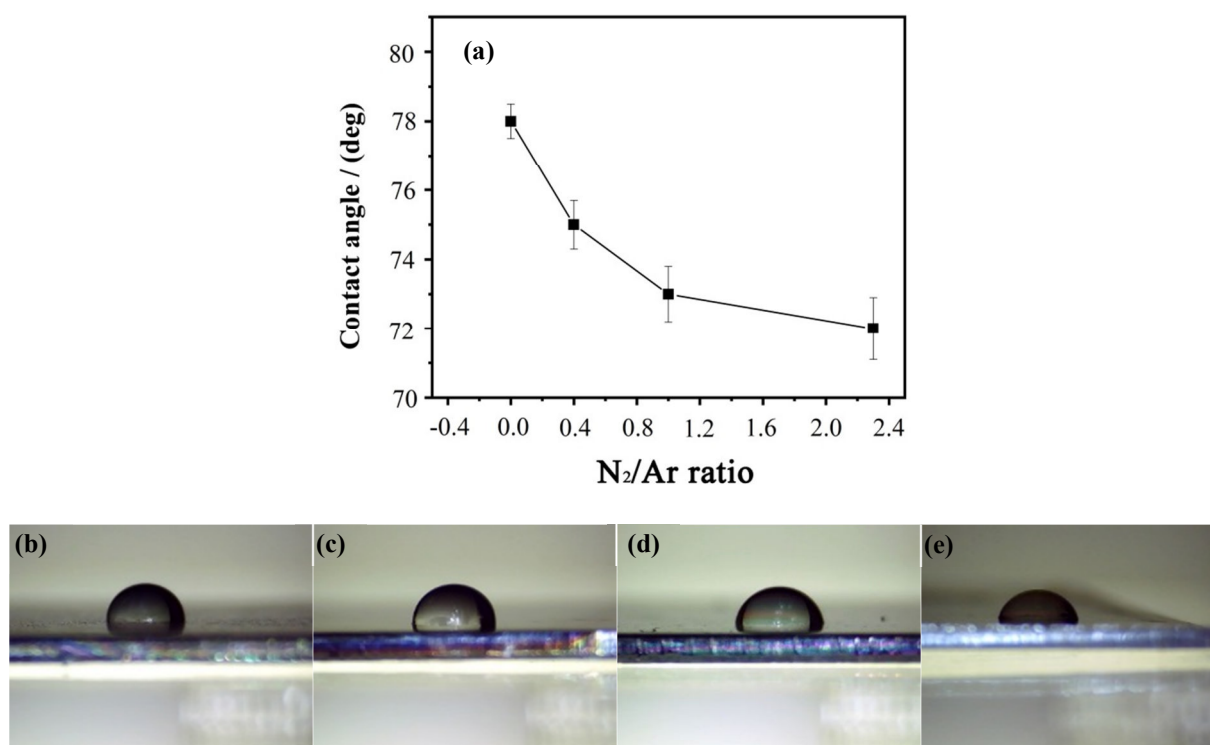


**Figure 5:** Contact angle of Cu: a-C: N thin coatings (a), C-1 (b), C-2 (c), C-3 (d) and C-4 (e) in interaction with a water drop.

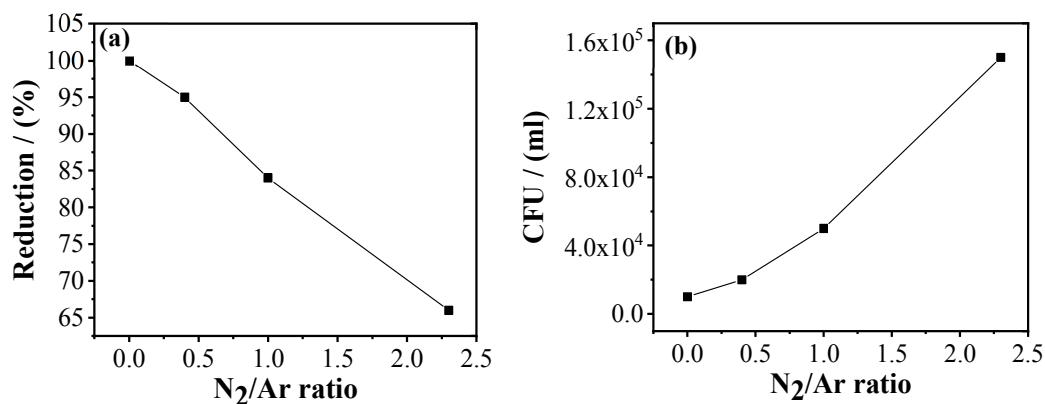


**Figure 6:** Variation of (a) *E. coli* deactivation percent and (b) sum of CFUs of Cu: a-C: N coated TC4 alloy.

Having assessed structure, morphology and surface properties of the coatings and antibacterial behavior, mechanical properties seem to be the last but not the least investigation of the coatings. Amongst these properties, coating's internal stress is a critical parameter in the field of functional thin films. Because it can directly affect film adhesion. Very high internal stress provides adequate energy for initiation and propagation of microcracks that will probably lead to detachment of the coatings from the substrate [40-43].

The internal stress values are given in Figure 7. The stress values are entirely compressive. An apparent increase can be observed by increasing the  $N_2/Ar$  ratio. Thus it can be assumed that coatings adhesion worsens as the nitrogen content increases.

Coatings' hardness and Young's modulus dependence on the  $N_2/Ar$  ratio is displayed in Figure 8 (a, b). The hardness varies across 11 to 24, and Young's modulus ranges from 150 to 300 GPa. The hardness of the coatings increases as  $N_2/Ar$  ratio rises

when Young's modulus increases with increasing  $N_2/Ar$  ratio getting to its highest value at  $N_2/Ar$  ratio of 1 and decreases for higher  $N_2/Ar$  ratio. To explain this behavior, the coatings morphology and internal stress values of a-C based coatings must be considered. As

shown in Figure 4, coatings prepared under higher  $N_2/Ar$  ratios demonstrate smooth and low defective structures, leading to higher hardness. Besides, higher internal stress also leads to higher hardness of the coatings [44-48].

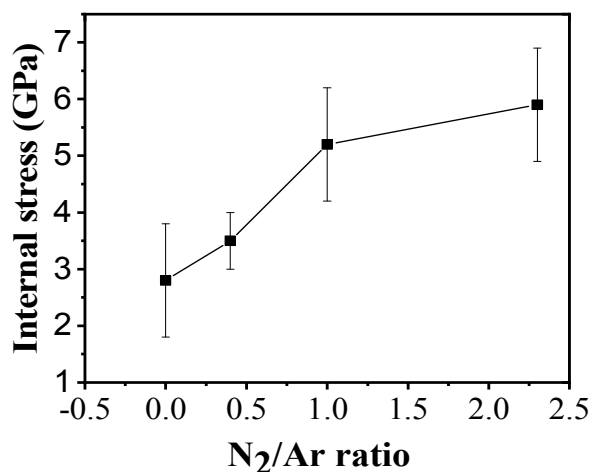


**Figure 7:** Variation of internal stress (compressive) value of Cu: a-C: N protective coatings with  $N_2/Ar$  ratio.

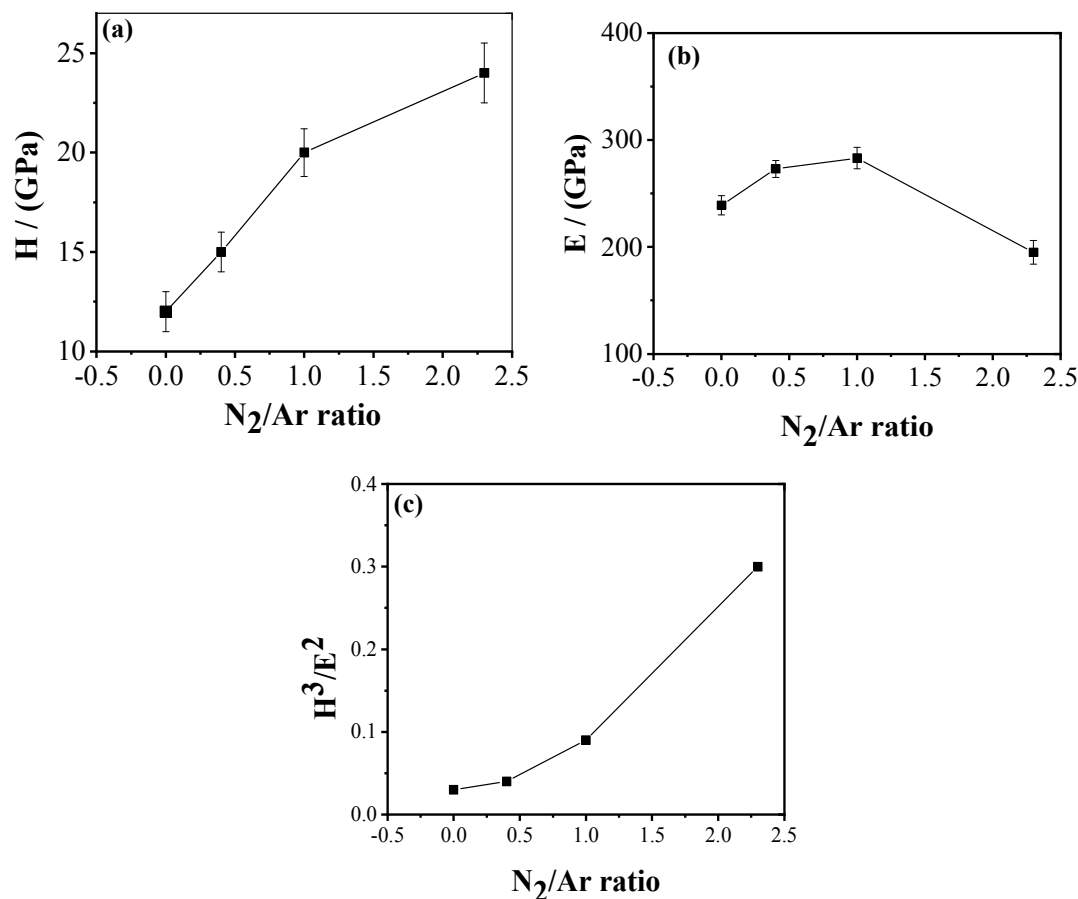


**Figure 8:** (a) Plastic hardness (H), (b) Young's modulus (E), and (c)  $H^3/E^2$  of Cu: a-C: N protective thin layers with  $N_2/Ar$  ratio.

To estimate the tribological characteristics of the coatings, the  $H^3/E^2$  ratio versus the  $N_2/Ar$  ratio is sketched, and shown in Figure 8. The  $H^3/E^2$  ratio reveals the plastic deformation resistance of a coating [49, 50]. It can be perceived that the  $H^3/E^2$  ratio of the coatings demonstrates an ascending trend as a function of the  $N_2/Ar$ . High hardness, low Young's modulus, and high  $H^3/E^2$  of the coatings containing higher nitrogen contents are assumed as typical properties of nanocomposite coatings [8, 30, 51]. Hence, it can be concluded that the desired mixture of mechanical characteristics and tribological properties of the Cu: a-C: N thin coatings have been obtained.

#### 4. Conclusions

The results demonstrated that the  $N_2/Ar$  ratio is a crucial deposition parameter that influences

microstructure, bactericide, and mechanical characteristics of hydrogen-free Cu: a-C: N coatings. Cu: a-C: N thin coatings readied at higher  $N_2/Ar$  ratios had a higher fraction of  $sp^3$  carbon. The higher fraction of  $sp^3$  carbon improved the mechanical characteristics of the coatings due to the strong  $\sigma$  bond of the adjacent carbon atoms. However, higher nitrogen content did not have a positive impact on antibacterial properties, although the coatings still exhibited good antibacterial resistance. The low bactericide characteristics of Cu: a-C: N coatings controlled by Cu content, and/or higher fraction of  $sp^3$  bonding. The outcomes of the present study confirmed that it is conceivable to tailor mechanical properties and bactericide properties of these coatings by manipulating the nitrogen content of the coatings to make them appropriate for the specific applications.

#### 5. References

1. E. Broitman, W. Macdonald, N. Hellgren, G. Radnoczi, A. Wennerberg, M. Jacobsson, L. Hultman, Carbon nitride films on orthopedic substrates, *Diam. Relat. Mater.*, 9(2000), 1984–1991.
2. P. Campbell, S. Ma, Y. H. Isolation of predominantly submicron-sized UHMWPE wear partick from periprosthetic tissues, *J. Biomed. Mater. Res.*, 29(1995), 127–131.
3. K. Bosdorf, I. Mollenhauer, G. Willmann, U. Boenick, Materials for hip joint prostheses - Alternatives to standard materials, *Biomed. Tech.*, 40(1995), 356–362.
4. M. Shinohara, H. Kawazoe, T. Inayoshi, T. aki Kawakami, Y. Matsuda, H. Fujiyama, Y. Nitta, T. Nakatani, Difference of deposition process of an amorphous carbon film due to source gases, *Thin Solid Films*, 518(2010), 3497–3501.
5. T. T. Liao, T. F. Zhang, S. S. Li, Q. Y. Deng, B. J. Wu, Y. Z. Zhang, Y. J. Zhou, Y. B. Guo, Y. X. Leng, N. Huang, Biological responses of diamond-like carbon (DLC) films with different structures in biomedical application, *Mater. Sci. Eng. C.*, 69(2016), 751–759.
6. M. Azzi, P. Amirault, M. Paquette, J. E. Klemberg-Sapieha, L. Martinu, Corrosion performance and mechanical stability of 316L/DLC coating system: Role of interlayers, *Surf. Coatings Technol.*, 204(2010), 3986–3994.
7. M. R. Derakhshandeh, M. J. Eshraghi, M. M. Hadavi, M. Javaheri, S. Khamseh, M. G. Sari, P. Zarrintaj, M.R. Saeb, M. Mozafari, Diamond-like carbon thin films prepared by pulsed-DC PE-CVD for biomedical applications, *Surf. Innov.*, 6(2018), 167–175.
8. D. G. Liu, J. P. Tu, R. Chen, C. D. Gu, Microstructure, corrosion resistance and biocompatibility of titanium incorporated amorphous carbon nitride films, *Surf. Coatings Technol.*, 206(2011), 165–171.
9. A. Nemati, M. Saghafi, S. Khamseh, E. Alibakhshi, P. Zarrintaj, M.R. Saeb, Magnetron-sputtered  $Ti_{1-x}Ni_x$  thin films applied on titanium-based alloys for biomedical applications: Composition-microstructure-property relationships, *Surf. Coatings Technol.*, 349(2018), 251–259.
10. Y. H. Chan, C. F. Huang, K. L. Ou, P. W. Peng, Mechanical properties and antibacterial activity of copper doped diamond-like carbon films, *Surf. Coatings Technol.*, 206(2011), 1037–1040.
11. M. Fedel, A. Motta, D. Maniglio, C. Migliaresi, Surface properties and blood compatibility of commercially available diamond-like carbon coatings for cardiovascular devices, *J. Biomed. Mater. Res. Part B Appl. Biomater.*, 90B(2008), 338–349.
12. M. Yoshida, S. Watanabe, T. Tanaka, T. Takagi, M. Shinohara, J.W. Lee, Investigation of diamond-like carbon formed on PET film by plasma-source ion implantation using  $C_2H_2$  and  $CH_4$ , *Nucl. Instruments Methods Phys. Res. Sect. B Beam Interact. with Mater. Atoms.*, 206(2003), 712–716.
13. A. Erdemir, I. B. Nilufer, O. L. Eryilmaz, M. Beschliesser, G. R. Fenske, Friction and wear performance of diamond-like carbon films grown in various source gas plasmas, *Surf. Coatings Technol.*, 120-121(1999), 589-593.
14. D. Bootkul, B. Supsermpol, N. Saenphinit, C.

- Aramwit, S. Intarasiri, Nitrogen doping for adhesion improvement of DLC film deposited on Si substrate by Filtered Cathodic Vacuum Arc (FCVA) technique, *Appl. Surf. Sci.*, 310(2014), 284-292.
15. M. H. Ahmed, J. A. Byrne, Effect of surface structure and wettability of DLC and N-DLC thin films on adsorption of glycine, *Appl. Surf. Sci.*, 258(2012), 5166-5174.
  16. N. Hellgren, M. Johansson, E. Broitman, L. Hultman, J. E. Sundgren, Role of nitrogen in the formation of hard and elastic CN<sub>x</sub> thin films by reactive magnetron sputtering, *Phys. Rev. B.*, 59(1999), 5162-5169.
  17. E. C. Cutiongco, D. Li, Y. W. Chung, C. S. Bhatia, Tribological Behavior of Amorphous Carbon Nitride Overcoats for Magnetic Thin-Film Rigid Disks, *J. Tribol.*, 118(1996), 543-548.
  18. A. Khurshudov, K. Kato, S. Daisuke, A. Khurshudov, K. Kato, S. Daisuke, Comparison of tribological properties of carbon and carbon nitride protective coatings over magnetic media, *J. Vac. Sci. Technol. A Vacuum, Surfaces, Film.*, 14(1996), 2935-2939.
  19. I. Ivanov, J. E. Greene, E. Broitman, W. T. Zheng, H. Sjo, N. Instruments, Stress development during deposition of CN<sub>x</sub> thin films, *Appl. Phys. Lett.*, 72(1998), 2532-2534.
  20. B. Pandey, P. P. P. Pal, S. Bera, S. K. K. Ray, A. K. K. Kar, Effect of nickel incorporation on microstructural and optical properties of electrodeposited diamond like carbon (DLC) thin films, *Appl. Surf. Sci.*, 261(2012), 789-799.
  21. S. Khamseh, E. Alibakhshi, M. Mahdavian, M. R. Saeb, H. Vahabi, J.-S. Lecomte, P. Laheurte, High-performance hybrid coatings based on diamond-like carbon and copper for carbon steel protection, *Diam. Relat. Mater.*, 80(2017), 84-92.
  22. S. Khamseh, E. Alibakhshi, M. Mahdavian, M. R. Saeb, H. Vahabi, N. Kokanyan, P. Laheurte, Magnetron-sputtered copper/diamond-like composite thin films with super anti-corrosion properties, *Surf. Coatings Technol.*, 333(2018), 148-157.
  23. S. Khamseh, E. Alibakhshi, B. Ramezanzadeh, M.G. Sari, A.K. Nezhad, Developing a graphite like carbon:niobium thin film on GTD-450 stainless steel substrate, *Appl. Surf. Sci.*, 511(2020), 145613.
  24. S. Khamseh, E. Alibakhshi, B. Ramezanzadeh, J. S. Lecomte, P. Laheurte, X. Noirefalize, F. Laoutid, H. Vahabi, Tailoring hardness and electrochemical performance of TC4 coated Cu/a-C thin coating with introducing second metal Zr, *Corros. Sci.*, 172(2020), 108713.
  25. J. S. Chen, S. P. Lau, G. Y. Chen, Z. Sun, Y. J. Li, B. K. Tay, J. W. Chai, Deposition of iron containing amorphous carbon films by filtered cathodic vacuum arc technique, *Diam. Relat. Mater.*, 10(2001), 2018-2023.
  26. N. Pasaja, S. Sansongsiri, S. Intarasiri, T. Vilaithong, A. Anders, Mo-containing tetrahedral amorphous carbon deposited by dual filtered cathodic vacuum arc with selective pulsed bias voltage, *Nucl. Instruments Methods Phys. Res. Sect. B Beam Interact. Mater. Atoms.*, 259(2007), 867-870.
  27. A. T. T. Koh, J. Hsieh, D. H. C. Chua, Structural characterization of dual-metal containing diamond-like carbon nanocomposite films by pulsed laser deposition, *Diam. Relat. Mater.*, 19(2010), 637-642.
  28. K. Page, I. P. Parkin, Antimicrobial surfaces and their potential in reducing the role of the inanimate environment in the incidence of hospital-acquired infections, *J. Mater. Chem.*, 19(2009), 3819-831.
  29. K. Page, R. G. Palgrave, I. P. Parkin, M. Wilson, L. P. Savin, A. V. Chadwick, Titania and silver-titania composite films on glass- potent antimicrobial coatings, *J. Mater. Chem.*, 17(2007), 95-104.
  30. N. Dwivedi, S. Kumar, H. K. Malik, C. Sreekumar, S. Dayal, C. M. S. Rauthan, O. S. Panwar, Investigation of properties of Cu containing DLC films produced by PECVD process, *J. Phys. Chem. Solids.*, 73(2012), 308-316.
  31. M. Grischke, K. Bewilogua, K. Trojan, H. Dimigen, Application-oriented modifications of deposition processes for diamond-like-carbon-based coatings, *Surf. Coat. Technol.*, 74-75(1995), 739-745.
  32. F. Heidenau, W. Mittelmeier, R. Detsch, M. Haenle, F. Stenzel, A novel antibacterial titania coating : Metal ion toxicity and in vitro surface colonization, *J. Mater. Sci. Med. J. Mater. Sci. Med.*, 6(2005), 883-888.
  33. A. Malesevic, R. Vitchev, K. Schouteden, A. Vanhulsel, C. Van Haesendonck, Synthesis of few-layer graphene via microwave plasma-enhanced chemical, *Nanotechnol.*, 19(2008), 305604-305609.
  34. H. Hasan, V. Abdelsayed, A. Kheder, K. AbouZeid, J. Terner, M. El-Shall, S. Al-Resayes, A. El-Azhary, Microwave synthesis of graphene sheets supporting metal nanocrystals in aqueous and organic media, *J. Mater. Sci.*, 19(2009), 3832-3837.
  35. L. Hultman, J. Neidhardt, N. Hellgren, H. Sjöström, J. E. Sundgren, Fullerene-like Carbon Nitride: A Resilient Coating Material, *MRS Bull.*, 28(2003), 194-202.
  36. C. Zou, W. Xie, X. Tang, Further improvement of mechanical and tribological properties of Cr-doped diamond-like carbon nanocomposite coatings by N codoping, *Jpn. J. Appl. Phys.*, 55(2016), 115501.
  37. E. Alibakhshi, E. Ghasemi, M. Mahdavian, B. Ramezanzadeh, Fabrication and characterization of layered double hydroxide/silane nanocomposite coatings for protection of mild steel, *J. Taiwan Inst. Chem. Eng.*, 80(2017), 924-934.
  38. R. Samiee, B. Ramezanzadeh, E. Alibakhshi, Corrosion inhibition performance and healing ability of a hybrid silane coating in the presence of praseodymium (III) cations, *J. Electrochem. Soc.*, 165(2018), 777-786.
  39. R. Samiee, B. Ramezanzadeh, M. Mahdavian, E. Alibakhshi, Assessment of the smart self-healing corrosion protection properties of a water-base hybrid organo-silane film combined with non-toxic organic/inorganic environmentally friendly corrosion

- inhibitors on mild steel, *J. Clean. Prod.*, 220(2019), 340-356.
40. J. H. Choi, H. S. Ahn, S. C. Lee, K. R. Lee, Stress reduction behavior in metal-incorporated amorphous carbon films : first-principles approach, *J. Phys. Conf. Ser.*, 29(2006), 155-158.
  41. M. Y. Ming, X. Jiang, D. G. Piliptsov, Y. Zhuang, A. V. Rogachev, A. S. Rudenkov, A. Balmakou, Chromium-modified a-C films with advanced structural, mechanical and corrosive-resistant characteristics, *Appl. Surf. Sci.*, 379(2016), 424-432.
  42. E. Broitman, W. T. Zheng, H. Sjöström, I. Ivanov, J. E. Greene, J. E. Sundgren, Stress development during deposition of CN<sub>x</sub> thin films, *Appl. Phys. Lett.*, 72(1998), 2532-2534.
  43. P. Couvrat, M. Denis, M. Langer, S. Mitura, P. Niedzielski, J. Marciniak, The corrosion tests of amorphous carbon coatings deposited by r.f. dense plasma onto steel with different chromium contents, *Diam. Relat. Mater.*, 4(1995), 1251-1254.
  44. C. T. Chuang, C. K. Chao, R. C. Chang, K. Y. Chu, Effects of internal stresses on the mechanical properties of deposition thin films, *J. Mater. Process. Technol.*, 201(2008), 770-774.
  45. D. T. Quinto, A. T. Santhanam, P. C. Jindal, Mechanical properties, structure and performance of chemically vapor-deposited and physically vapor-deposited coated carbide tools, *Mater. Sci. Eng.*, 105-106(1988), 443-452.
  46. J. Gunnars, A. Alahelisten, Thermal stresses in diamond coatings and their influence on coating wear and failure, *Surf. Coatings Technol.*, 80(1996), 303-312.
  47. A. Mani, P. Aubert, F. Mercier, H. Khodja, C. Berthier, P. Houdy, Effects of residual stress on the mechanical and structural properties of TiC thin films grown by RF sputtering, *Surf. Coatings Technol.*, 194(2005), 190-195.
  48. M. Bai, K. Kato, N. Umehara, Y. Miyake, Nanoindentation and FEM study of the effect of internal stress on micro r nano mechanical property of thin CN<sub>x</sub> films, *Thin Films*, 377-378(2000), 138-147.
  49. P. Kulu, R. Veinthal, M. Saarna, R. Tarbe, Surface fatigue processes at impact wear of powder materials, *Wear*, 263(2007), 463-471.
  50. P. Kulu, I. Hussainova, R. Veinthal, Solid particle erosion of thermal sprayed coatings, *Wear.*, 258(2005), 488-496.
  51. J. Musil, H. Poláková, Hard nanocomposite Zr-Y-N coatings, correlation between hardness and structure, *Surf. Coatings Technol.*, 127(2000), 99-106.

How to cite this article:

S. Khamseh, M. Ganjaee Sari, E. Alibakhshi, M. Nemati Valandaran, Hydrogen-free Cu: Amorphous-C: N coating on TC4 Titanium Alloy: The Role of Gas Ratio on Mechanical and Antibacterial Potency. *Prog. Color Colorants Coat.*, 14 (2021), 281-291.

